

**Balanced Convective Circulations in a Stratified Atmosphere. Part I:
A Framework for Assessing Radiation, the Coriolis Force, and Drag**

David H. Marsico,^a Joseph A. Biello,^a Matthew R. Igel^b

^a *Department of Mathematics, University of California Davis, Davis, California*

^b *Department of Land, Air and Water Resources, University of California Davis, Davis, California*

⁶ Corresponding author: David H. Marsico, dhmarsico@ucdavis.edu

7 ABSTRACT: The so-called traditional approximation, wherein the component of the Coriolis
8 force proportional to the cosine of latitude is ignored, is frequently made in order to simplify the
9 equations of atmospheric circulation. For velocity fields whose vertical component is comparable
10 to their horizontal component (such as convective circulations), and in the tropics where the sine
11 of latitude vanishes, the traditional approximation is not justified. We introduce a framework for
12 studying the effect of diabatic heating on circulations in the presence of both traditional and non-
13 traditional terms in the Coriolis force. The framework is intended to describe steady convective
14 circulations on an f-plane in the presence of radiation and momentum damping. We derive a
15 single elliptic equation for the horizontal velocity potential, which is a generalization of the weak
16 temperature Gradient (WTG) approximation. The elliptic operator depends on latitude, radiative
17 damping, and momentum damping coefficients. We show how all other dynamical fields can be
18 diagnosed from this velocity potential; the horizontal velocity induced by the Coriolis force has a
19 particularly simple expression in terms of the velocity potential. Limiting examples occur at the
20 equator, where only the non-traditional terms are present, at the poles, where only the traditional
21 terms appear, and in the absence of radiative damping where the WTG approximation is recovered.
22 We discuss how the framework will be used to construct dynamical, nonlinear convective models,
23 in order to diagnose their consequent upscale momentum and temperature fluxes.

24 **1. Introduction**

25 The full Coriolis force contains terms proportional to the sine and cosine of latitude. The former
26 are referred to as the traditional Coriolis terms, and couple the zonal and meridional momentum
27 equations. The latter, referred to as the non-traditional Coriolis terms (NCTs), couple the zonal
28 and vertical momentum equations. Scaling arguments have often been used to justify the neglect
29 of the NCTs. For instance, in midlatitude, synoptic scale meteorology, it can be shown that the
30 non-traditional Coriolis term in the zonal momentum equation is relatively small, and in the vertical
31 momentum equation, it is negligible compared to vertical accelerations, gravity, and the vertical
32 pressure gradient. Under these circumstances, the “traditional approximation” is made, whereby
33 the NCT are neglected but the traditional Coriolis terms (TCT) are retained. However, near the
34 equator, the cosine and sine of latitude approach unity and zero, respectively, and it becomes more
35 difficult to justify the outright neglect of the non-traditional terms for circulations which are not in
36 hydrostatic balance.

37 The effect of the non-traditional Coriolis terms have been studied in different contexts. They have
38 been considered in convection (Igel and Biello 2020), tropical waves (Ong and Roundy 2020; Ong
39 and Yang 2022), convective momentum transport (LeMone 1983), oceanic dynamics (Marshall
40 and Schott 1999), and idealized studies of the planetary boundary layer (Dubos et al. 2008). The
41 work of Igel and Biello (2020) shows how the NCT and the pressure field induced by convective
42 circulations create a purely horizontal force which acts on the circulation. In the framework
43 described below, this horizontal force will manifest as a secondary horizontal circulation added
44 to the primary convective circulation. The non-traditional Coriolis terms have also shown to be
45 important in shallow water approximations (Stewart and Dellar 2013, 2012, 2010). In addition, a set
46 of equations that retain the non-traditional Coriolis terms, and possess conservation principles for
47 mass, energy, and potential vorticity were derived in Tort and Dubos (2014). However, it is largely
48 the case that the influence of the NCTs on atmospheric flows remains incompletely understood and
49 poorly appreciated. Studies of the non-traditional terms tend to conclude that, when considered
50 diligently, the NCTs should not be ignored in low-latitude meteorological situations with the
51 potential for or the occurrence of sustained vertical motion.

52 Our original intention for this work was to study the NCTs only in a broad way. We wanted to
53 introduce a mathematical framework for understanding tropical dynamics under the influence of the

54 NCTs that would be applicable from the synoptic scales to the mesoscales and would not necessarily
55 invoke wave dynamics, the latter having been the focus of most previous work on the NCTs. To do
56 so, we introduced a scaling of the incompressible Euler equations on an equatorial beta-plane that
57 would allow us to study the NCTs' effect on the corresponding steady state equations. However, we
58 realized that our analysis could easily be extended to the Euler equations at an arbitrary latitude,
59 and the case where only the non-traditional terms are present could be obtained by evaluating the
60 theory at zero latitude.

61 To yield a general, albeit linear, framework, we consider the impacts of radiation and dissipa-
62 tion of momentum on the dynamics. The latter allows the possibility of steady state solutions.
63 Consideration of the former is motivated by mesoscale studies of tropical systems which tend to
64 emphasize the important role of radiation, especially in horizontal gradients of radiative heating
65 (Wing et al. 2017), and by its fundamental role in the energy balance of the tropical atmosphere
66 (Manabe and Strickler 1964). As a consequence of our choice of time and length scales, and in the
67 absence of radiation, there is a simplification of our equations that yields one of the fundamental
68 features of the weak temperature gradient (WTG) approximation: the direct diagnosis of vertical
69 velocity from the heating. The WTG approximation has been applied on mesoscales and synoptic
70 scales in the tropics to understand, among other things, tropical cyclone formation (Raymond et al.
71 2007; Adames et al. 2021), the Madden-Julian Oscillation (Chikira 2014), and the Walker Cell
72 (Bretherton and Sobel 2002). At first glance, it may be counterintuitive that convection can be
73 described by a diagnostic equation for the vertical velocity, since it is understood to be achieved on
74 meso and synoptic scales in the tropics. However, balance of the form of WTG requires that the
75 waves travel across the region of interest more quickly than the circulation transports the fluid. In
76 this framework, the gravity wave travel time across an isolated convective element is much faster
77 than a convective turnover time, which are the timescales under consideration. This time scale
78 separation means that gravity waves quickly re-stratify the potential temperature (or buoyancy) in
79 the vicinity of the convection, so that the time derivative of the buoyancy equation can be neglected
80 in favor of its balanced state (a radiation modified version of WTG). A WTG balance on convective
81 scales was first developed by Klein and collaborators and was summarized nicely by (Klein 2010).
82 More recently, a diagnostic equation for the vertical velocity in deep convection was also derived
83 by (Hittmeir and Klein 2018) using the method of asymptotic scale analysis.

84 The derivation of our framework will begin with a nondimensionalization and scale analysis, but
85 will set aside a systematic asymptotic analysis for the future. We split our work into two parts. Here
86 in Part I, we derive sets of diagnostic equations for velocity, pressure, and buoyancy perturbation.
87 We consider three distinct cases to elucidate the effect of the Coriolis force on convective flows;
88 when the full Coriolis force, only the non-traditional terms, or only the traditional terms are
89 retained. The last two cases occur at the equator and pole, respectively. Since the equatorial,
90 non-traditional Coriolis case is of the most interest to us, it is presented fully in Part II (Marsico
91 et al. In Preparation).

92 This paper is organized as follows. In section 2, we discuss the velocity, and time scales for which
93 the incompressible Euler equations yield solutions corresponding to equilibrated circulations on
94 atmospheric convective length scales, as would be used for sub-grid convective parameterizations
95 in large scale computations. Since this is a preliminary framework, we focus on flow strengths
96 that can be described by linear theory because they are weak enough. The effects of turbulent
97 dissipation on sub-grid scales are often approximated by drag damping, or enhanced, turbulent
98 diffusivity. In our model, we will use linear dissipation on convective scales to account for the
99 enhanced diffusivity associated with sub-grid turbulence. We also focus on time scales where
100 the zonal and meridional components of the full Coriolis force balance the pressure gradients
101 and damping, while the vertical component balances the vertical pressure gradient, damping, and
102 buoyancy.

103 In order to solve the resulting steady linear equations, it is necessary to introduce damping, and
104 we consider two forms: first, constant drag damping in the momentum, and Newtonian cooling
105 in the buoyancy equations; second, diffusive damping in the momentum equations and Newtonian
106 cooling in the buoyancy equation. In section 3, we use the Helmholtz decomposition to separate the
107 velocity field into two components. The poloidal component of the velocity field is horizontally
108 convergent and directly responds to the heating; we thus describe it as the primary circulation
109 (Zhang and Schubert 1997). A purely horizontal velocity field is generated from the poloidal
110 circulation, the Coriolis force, and the momentum damping; we describe it as the secondary
111 circulation.

112 There are two significant physical predictions of our framework regarding the effect of NCT
113 and radiation. The first is expressed by equation (18), which arises as a balance between the “net

114 Coriolis force" (Igel and Biello 2020) and momentum damping. It provides a simple relationship
115 between the vertical derivative of the stream function of the secondary circulation and the derivative
116 of the potential function of the primary (poloidal) circulation along the axis of rotation of the Earth.
117 The second is expressed in equation (19), where the potential of the primary, poloidal circulation is
118 related to the latent heating through an elliptic operator. In the absence of radiation, this expression
119 reduces to the weak temperature gradient approximation; that is to say, the vertical velocity is
120 proportional to the latent heating. Radiation allows the effect of latent heating to be felt away from
121 its source, thereby providing a mechanism for descent or ascent away from the center of convection.
122 In section 4, we contrast solutions to these equations at the equator (purely NCT) versus the poles
123 (purely TCT). In section 5, our results are summarized.

124 **2. Length and time scales of the Primitive Equations appropriate to convective circulations**

125 Our framework describes steady, convective circulations under the influence of buoyancy, NCT,
126 TCT, and damping. In this and our companion manuscript the framework will be linear. Our
127 reasoning is that nonlinearity will primarily create turbulent dissipation (modelled as a linear
128 damping), and can be mostly accounted for by eddy diffusivity. Future work will extend these
129 results to circulations where advective nonlinearities cannot be neglected, yet the weak temperature
130 gradient will be maintained. It is the versatility of the WTG simplification that allows for simple
131 solutions in both linear and nonlinear steady circulations. Furthermore, in the linear regime, the
132 various properties of the circulation and buoyancy response to diabatic heating can be straightfor-
133 wardly associated with their sources and sinks, making this framework a natural starting point for
134 a dynamical convective parameterization.

135 In the following paragraphs, we non-dimensionalize the equations of motion and describe the
136 relevant spatial, temporal, velocity and buoyancy scales. Although we will ultimately work with
137 a linear and dimensional model, the discussion of non-dimensionalization is important to ensure
138 our framework remains consistent with flows we seek to describe. Furthermore, we envision this
139 framework as the first step toward a multi-scale analysis of the nonlinear effects of convection on
140 meso- and synoptic scale circulations in keeping with (Klein 2010), (Hittmeir and Klein 2018), and
141 (Hirt et al. 2023). A careful multi-scale analysis must begin with a clear non-dimensionalization

142 of the equations of motion in order to identify the relevant small parameters used in the asymptotic
 143 method. Therefore, with an eye to future applications, we proceed with the scale analysis.

144 We begin with the incompressible, stratified, damped Euler equations on an f-plane at a latitude
 145 λ ,

$$\frac{\partial u}{\partial t} + \mathbf{u} \cdot \nabla u - 2\Omega v \sin(\lambda) + 2\Omega \cos(\lambda) w = -\frac{\partial \phi}{\partial x} - d_1 u, \quad (1a)$$

$$\frac{\partial v}{\partial t} + \mathbf{u} \cdot \nabla v + 2\Omega u \sin(\lambda) = -\frac{\partial \phi}{\partial y} - d_1 v, \quad (1b)$$

$$\frac{\partial w}{\partial t} + \mathbf{u} \cdot \nabla w - 2\Omega u \cos(\lambda) = -\frac{\partial \phi}{\partial z} + b - d_1 w, \quad (1c)$$

$$\frac{Db}{Dt} + N^2 w = S \quad (1d)$$

$$\nabla \cdot \mathbf{u} = 0, \quad (1e)$$

146 where $b = g\theta/\theta_0$ is the buoyancy perturbation, θ is the potential temperature perturbation, θ_0 is a
 147 reference potential temperature, d_1 is the damping coefficient due to the sub-cloud scale turbulent
 148 dissipation (or damping operator, if e.g. a drag parameterization is used), $N^2 = (g/\theta_0)(d\tilde{\theta}/dz)$ is
 149 the squared buoyancy frequency of the unperturbed atmosphere, $\tilde{\theta}(z)$ is the background potential
 150 temperature stratification, and $\phi = p/\rho_0 + gz$ is the Montgomery potential for a constant density
 151 fluid, ρ_0 . The buoyancy source is related to the diabatic heating through $S = (g/\theta_0)S_\theta$. Since we
 152 consider an idealized theoretical framework, we use the incompressible equation (1e), instead of
 153 the anelastic continuity equation.

154 To non-dimensionalize the equations, we introduce the length, time, velocity, buoyancy, pressure
 155 and latent heating scales, $(L, T, U, b_0, \phi_0, S_0)$, as follows: $(x, y, z) = L(x', y', z')$, $t = Tt'$, $(u, v, w) =$
 156 $U(u', v', w')$, $b = b_0 b'$, $\phi = \phi_0 \phi'$, and $S = S_0 S'$. Since the scaling is isotropic in the vertical
 157 and horizontal directions, the resulting vertical momentum equation will not express hydrostatic
 158 balance. Instead we allow for the possibility that all of the linear forces participate in the dominant
 159 balance at lowest order. Rewriting equations (1a)-(1e) in terms of the non-dimensional variables

160 (and dropping primes for readability) we find

$$\frac{\partial u}{\partial t} + \frac{UT}{L} \mathbf{u} \cdot \nabla u - 2\Omega T \sin(\lambda) v + 2\Omega T \cos(\lambda) w = -\frac{\phi_0 T}{LU} \frac{\partial \phi}{\partial x} - d_1 T u, \quad (2a)$$

$$\frac{\partial v}{\partial t} + \frac{UT}{L} \mathbf{u} \cdot \nabla v + 2\Omega T \sin(\lambda) u = -\frac{\phi_0 T}{LU} \frac{\partial \phi}{\partial y} - d_1 T v, \quad (2b)$$

$$\frac{\partial w}{\partial t} + \frac{UT}{L} \mathbf{u} \cdot \nabla w - 2\Omega T \cos(\lambda) u = \frac{\phi_0 T}{LU} \left(-\frac{\partial \phi}{\partial z} + \frac{b_0 L}{\phi_0} b \right) - d_1 T w, \quad (2c)$$

$$\frac{b_0}{N^2 U T} \left[\frac{\partial b}{\partial t} + \frac{UT}{L} \mathbf{u} \cdot \nabla b \right] + w = \frac{S_0}{N^2 U} S \quad (2d)$$

$$\nabla \cdot \mathbf{u} = 0. \quad (2e)$$

161 As with all asymptotically inspired methods, one attains a simplified model by seeking a dominant
 162 balance between different terms in the primitive equations. However, the vertical and horizontal
 163 length scales under consideration are fixed by the troposphere height. Choosing $L = 7\text{ km}$ allows
 164 for deep convective circulations (order $2L$) as well as developing convection (order $L/2$).

165 The Coriolis force participates in the dominant balance when $2\Omega T \geq 1$, which means that we
 166 consider time scales of $T = (2\Omega)^{-1} \approx 2\text{ hours}$ or larger. Notwithstanding that on a 2 hour time scale
 167 the time derivatives in the momentum equation may not necessarily be negligible, the balanced
 168 circulations we consider herein can be thought of as either the equilibration of a convective
 169 circulation under Coriolis and damping, or a quasi-stationary, slowly evolving circulation pattern
 170 due to latent heating.

171 The relative strength of the nonlinear terms to the linear terms is measured by the Rossby number

$$\frac{UT}{L} = \frac{U}{2\Omega L} \equiv \text{Ro}.$$

172 A linear regime is applicable if the Rossby number of the flow is less than one. So $\text{Ro} < 1$ implies
 173 the velocity U is less than the scale $2\Omega L \approx 1\text{ m/s}$. From the perspective of small scale turbulent
 174 motions in atmospheric convection, this is indeed a small velocity. However, we expect that this
 175 velocity scale is appropriate to the large scale envelope of convection, and that the smaller scale,
 176 faster motions contribute to the sub-cloud enhanced turbulent diffusion.

177 Buoyancy driven circulations of low Mach number (the ratio of the characteristic speed to
 178 the speed of sound) result in incompressible (or anelastic) velocity fields to a high degree of

179 approximation, and this is maintained by the pressure gradient. Therefore we expect that the
 180 buoyancy and pressure perturbation are the same order of magnitude, $b_0 = \phi_0/L$. Indeed this is
 181 often observed in simulated active convection (Jeevanjee and Romps 2016; Peters 2016). We also
 182 expect that the pressure gradient and buoyancy be of the same order of magnitude as the Coriolis
 183 force, thereby $\phi_0 = (UL)/T = \text{Ro}(L^2)/T^2$, which yields the buoyancy scale

$$b_0 = \text{Ro} \frac{L}{T^2}.$$

184

185 Using $UT = \text{Ro} L$ we can estimate the coefficient multiplying the temperature transport term on
 186 the left side of equation (2d) to be

$$\frac{b_0}{N^2 UT} = \frac{\text{Ro} L}{T^2} \frac{1}{N^2 \text{Ro} L} = (NT)^{-2} \equiv \epsilon^2,$$

187 where the last equality is the definition of ϵ . Since the Brunt Vaisala frequency in the troposphere
 188 is approximately $N = .02 \text{ s}^{-1}$, and using a Coriolis time scale $T \approx 7200 \text{ s}$ we find

$$\epsilon \approx \frac{1}{144},$$

189 so that the temperature advection term on the left hand side of (2d) is extremely small compared to
 190 the vertical transport of the background stratification (the w term on the left hand side of equation
 191 (2d)). Effectively this means that gravity waves are extremely fast compared with advection.
 192 Therefore, the weak temperature Gradient approximation, where the vertical velocity balances the
 193 diabatic heating in a diagnostic equation, is an excellent approximation even on convective scales.
 194 We also expect that the momentum damping will balance the Coriolis force, so that the damping
 195 rate, d_1^{-1} , is of the order $T \approx 2 \text{ hrs}$.

196 These scale arguments establish the time, length, and diabatic heating scales for which the linear,
 197 steady approximation provides an excellent description of the circulation. Convective circulations
 198 do not necessarily satisfy these constraints throughout their development, but the linear steady
 199 theory can still provide insights to the induced circulation, even if nonlinear advection would tend
 200 to slowly evolve such a circulation.

202 *a. Radiative Damping*

203 We are ultimately interested in the effect that radiative cooling has on steady state circulations
 204 and can model its effect by introducing a Newtonian cooling term of the form $-d_2 b$ to the right
 205 hand side of equation (1d). This term would then be non-dimensionalized as $-(d_2 b_0)/(N^2 U)b$
 206 on the right hand side of equation (2d). Inclusion of this radiative term in no way changes any
 207 of the previous scaling arguments. Now, if the diabatic heating source and radiative sink on the
 208 right hand side of the temperature equation are to be in balance with the vertical velocity, then
 209 $S_0 \approx d_2 b_0 \approx UN^2 = \text{Ro} \times 1 \text{ m/s} \times (.02 \text{ s}^{-1})^2 = 1.44 \text{ m/s}^2 \text{ hr}^{-1}$. At the small buoyancy perturbations
 210 considered here, this balance requires a somewhat large Newtonian cooling parameter, d_2 .

211 **3. Linear Convective WTG with full Coriolis force**

212 In this section we derive the framework of the Linear Convective WTG with the full Coriolis
 213 force. As we discussed above, we consider the linear, steady versions of equations (1a) - (1e) with
 214 a heating source and linear cooling in the temperature equation, and damping in the momentum
 215 equations. For the momentum equations, we will discuss both linear drag and enhanced turbulent
 216 diffusion.

217 In order to elucidate the physics of the problem, as well as simplify the mathematics, we will
 218 begin by using the Helmholtz decomposition to separate the horizontally convergent flow which
 219 directly responds to diabatic heating from the horizontally non-convergent flow which arises as
 220 a balance between the Coriolis force, and the momentum damping. The theory will consist of
 221 an elliptic (Poisson-like) equation for the horizontal velocity potential with a source term given
 222 by the diabatic heating. We will show how the other variables, the horizontal stream function,
 223 pressure, buoyancy, and the three components of the velocity, can all be diagnosed from this

224 velocity potential. The linear convective WTG equations with Coriolis force are

$$-2\Omega \sin(\lambda)v + 2\Omega \cos(\lambda)w = -\frac{\partial \phi}{\partial x} - d_1 u \quad (3a)$$

$$2\Omega \sin(\lambda)u = -\frac{\partial \phi}{\partial y} - d_1 v \quad (3b)$$

$$-2\Omega \cos(\lambda)u = -\frac{\partial \phi}{\partial z} + b - d_1 w \quad (3c)$$

$$N^2 w = S - d_2 b, \quad (3d)$$

$$\frac{\partial u}{\partial x} + \frac{\partial v}{\partial y} + \frac{\partial w}{\partial z} = 0, \quad (3e)$$

225 where d_1 is the momentum damping coefficient, and d_2 is the radiative damping coefficient. We
 226 first consider the case when d_1 and d_2 are due to Newtonian drag and radiative damping and then
 227 show how the theory can be easily extended to account for turbulent diffusion.

228 To describe the analytic solution of these equations, we follow the Helmholtz decomposition
 229 (Helmholtz 1867; Lebovitz 1989), introducing the stream function, ψ , and velocity potential, Φ ,
 230 and write the velocity field as

$$\mathbf{u} = (-\Phi_x - \psi_y)\mathbf{i} + (-\Phi_y + \psi_x)\mathbf{j} + w\mathbf{k} \quad (4)$$

231 The horizontally irrotational component, described by Φ , can converge in the horizontal direction
 232 (it was described as horizontally confluent in (Igel and Biello 2020)) and constitutes a poloidal
 233 vector field which is directly tied to the vertical velocity through a kinematic expression. The
 234 horizontally rotational component is described by a stream function, ψ , and therefore has no
 235 convergence in the horizontal plane. Its relationship to the velocity potential is a consequence of
 236 physics, as we will describe below. Setting the divergence of equation (4) to zero yields the well
 237 known Poisson equation for the velocity potential in terms of the vertical velocity

$$\nabla_h^2 \Phi = w_z, \quad (5)$$

238 where ∇_h^2 is the Laplacian operator in the horizontal (x, y) direction alone. Taking the vertical
 239 component of the curl of the velocity field, yields the (also) well known expression of the stream

²⁴⁰ function in terms of the vertical component of vorticity

$$\nabla_h^2 \psi = v_x - u_y. \quad (6)$$

²⁴¹ We now derive an equation for Φ in terms of S by eliminating the pressure and buoyancy from
²⁴² the momentum equations. We will then use equations (4)-(6) to write this equation in terms of Φ .
²⁴³ Differentiating equation (3a) with respect to z , and equation (3c) with respect to x and eliminating
²⁴⁴ ϕ yields

$$d_1 u_z - 2\Omega \sin(\lambda) v_z + 2\Omega \cos(\lambda) w_z = -2\Omega \cos(\lambda) u_x - b_x + d_1 w_x. \quad (7)$$

²⁴⁵ Differentiating equation (3b) with respect to z , equation (3c) with respect to y and eliminating ϕ
²⁴⁶ yields

$$2\Omega \sin(\lambda) u_z + d_1 v_z = -2\Omega \cos(\lambda) u_y - b_y + d_1 w_y. \quad (8)$$

²⁴⁷ Now we use equation (3d) to eliminate b from (7)

$$d_1 u_z - 2\Omega \sin(\lambda) v_z + 2\Omega \cos(\lambda) w_z = -2\Omega \cos(\lambda) u_x + \frac{N^2 w_x - S_x}{d_2} + d_1 w_x \quad (9)$$

²⁴⁸ and from equation (8)

$$2\Omega \sin(\lambda) u_z + d_1 v_z = -2\Omega \cos(\lambda) u_y + \frac{N^2 w_y - S_y}{d_2} + d_1 w_y. \quad (10)$$

²⁴⁹ Notice d_2 appears in the denominator in both equations (9) and (10), and this term would be
²⁵⁰ singular if d_2 were zero. In this limit, the WTG approximation is recovered for w and therefore Φ ,
²⁵¹ i.e. $N^2 w = S$. Upon differentiating equation (9) with respect to x , equation (10) with respect to y ,
²⁵² adding the results, taking the z -derivative, and making some rearrangements we obtain

$$d_1 (u_{xz} + v_{yz}) + 2\Omega \{ \sin(\lambda) (u_{yz} - v_{xz}) + \cos(\lambda) [w_{xz} + \nabla_h^2 u] \} = \frac{(N^2 + d_1 d_2) \nabla_h^2 w - \nabla_h^2 S}{d_2}. \quad (11)$$

²⁵³ Using the incompressibility constraint, (11) simplifies to

$$-d_1 d_2 w_{zz} - 2\Omega d_2 \{ \sin(\lambda) (v_{xz} - u_{yz}) + \cos(\lambda) [v_{xy} - u_{yy}] \} = (N^2 + d_1 d_2) \nabla_h^2 w - \nabla_h^2 S. \quad (12)$$

254 One can recognize the vertical component of vorticity, $v_x - u_y$, in both Coriolis terms on the left
 255 hand side of (12), which we will eliminate in favor of the Laplacian of the stream function. The
 256 vorticity is operated on by the derivative

$$\frac{\partial}{\partial n} \equiv \cos(\lambda) \frac{\partial}{\partial y} + \sin(\lambda) \frac{\partial}{\partial z}. \quad (13)$$

257 This is the directional derivative parallel to the direction of the North polar axis (thus our choice
 258 of ‘ n ’) as viewed from the tangent plane at latitude λ . A way to visualize this derivative is that, at
 259 an latitude λ , the derivative is taken in a direction which points toward the North Star. Taking the
 260 derivative of (12) with respect to z , we can use (5) to replace w in favor of Φ , and upon rearranging
 261 the expression we find

$$(N^2 + d_1 d_2) \nabla_h^4 \Phi + d_1 d_2 \nabla_h^2 \Phi_{zz} = \nabla_h^2 S_z - 2\Omega d_2 \nabla_h^2 \psi_{nz}. \quad (14)$$

262 Next, we invert one instance of the horizontal Laplacian throughout the expression (14). The re-
 263 sulting expression would have an arbitrary harmonic function, which is the kernel of the Laplacian,
 264 added to the right hand side. However, all harmonic functions either grow at infinity (corresponding
 265 to solutions growing away from the source) or are singular at a point in the domain (corresponding
 266 to solutions which blow up at a point). Therefore we can set the harmonic function to zero, and we
 267 arrive at one expression which relates the horizontal stream function, the horizontal convergence
 268 (potential Φ), and the diabatic heating

$$(N^2 + d_1 d_2) \nabla_h^2 \Phi + d_1 d_2 \Phi_{zz} = S_z - 2\Omega d_2 \psi_{nz}. \quad (15)$$

269 We have chosen to work with the potential for the horizontal convergence, Φ , in order to attain
 270 an expression which does not contain any horizontal derivatives of S . In the companion paper,
 271 we consider diabatic heating profiles with horizontal discontinuities, such as would be expected
 272 during cloud formation, and wish to avoid second derivatives of discontinuous functions. By
 273 setting $d_2 = 0$, we recover the WTG approximation from (15).

274 In order to construct a single elliptic PDE for Φ , we need another expression relating the stream
 275 function to the potential. Note that the derivatives we have used to arrive at (15) construct the

276 horizontal components of the vorticity equation. Subtracting the y -derivative of (3a) from the
 277 x -derivative of (3b) eliminates the horizontal pressure gradient and describes vertical component
 278 of the vorticity equation, which is not directly affected by buoyancy

$$2\Omega \{ \sin(\lambda) [u_x + v_y] - \cos(\lambda) w_y \} = -d_1 [v_x - u_y]. \quad (16)$$

279 Taking the z -derivative of (16) and replacing the components of the velocity with the stream
 280 function and potential

$$-2\Omega \{ \sin(\lambda) \nabla_h^2 \Phi_z + \cos(\lambda) \nabla_h^2 \Phi_y \} = -d_1 \nabla_h^2 \psi_z. \quad (17)$$

281 Again, using the expression for the directional derivative along the north polar axis, inverting an
 282 instance of the horizontal Laplacian on each term, and swapping the sides of the equality yields
 283 the extremely simple relationship relating the stream function to the velocity potential

$$d_1 \frac{\partial \psi}{\partial z} = 2\Omega \frac{\partial \Phi}{\partial n}. \quad (18)$$

284 Expression (18) is elegant, deceptively simple, and merits some elucidation. Although the
 285 right hand side is measured in units of acceleration, it arose from the vertical *torque* due to the
 286 Coriolis force acting on a poloidal velocity field described by Φ (Igel and Biello 2020). From the
 287 Helmholtz decomposition, the poloidal component of a velocity field is uniquely determined from
 288 its vertical component, yielding the convergence in the horizontal plane which compensates for
 289 the vertical circulation; that is to say it is the solution of equation (5) substituted into (4). This
 290 is a significant relationship between the convective, primary circulation described by Φ , and the
 291 horizontal, secondary circulation described by the stream function, ψ . Its derivation was motivated
 292 by the computation in (Igel and Biello 2020), of the divergence free portion of the Coriolis force
 293 induced by a convective velocity field. When this divergence free component of the Coriolis force
 294 is balanced by momentum drag (or dissipation), equation (18) results.

295 The left hand side of equation (18) arises from the damping of the vertical component of the
 296 vorticity. That vertical component of vorticity is, itself, due to the secondary circulation, described
 297 by ψ , in the horizontal plane (again refer to equation (4)). Therefore, equation (18) is the statement

298 that the vertical torque due to the Coriolis force acting on the convective circulation must be in
 299 balance with the torque associated with vorticity damping (later dissipation); in the absence of
 300 this damping ($d_1 = 0$) there is no balanced circulation. Since we have chosen to model damping
 301 linearly, then the response, ψ , corresponds to a secondary horizontal circulation which is linearly
 302 related to the primary poloidal (convective) circulation. That the secondary circulation is singular
 303 in the damping coefficient, d_1 , is notable, but not surprising given that equilibrium flow must be
 304 in, or nearly in, force balance. Ultimately, in any convective model, it will be the upscale fluxes
 305 of momentum, and thermodynamic quantities that are of interest to convective parameterizations,
 306 and we will discuss these fluxes in a subsequent manuscript.

307 We can now eliminate ψ from equation (15) using equation (18) to arrive at an elliptic equation
 308 for the velocity potential in terms of the diabatic heating

$$\nabla_h^2 \Phi + \frac{d_1 d_2}{N^2 + d_1 d_2} \left[\Phi_{zz} + \left(\frac{2\Omega}{d_1} \right)^2 \Phi_{nn} \right] = \frac{S_z}{(N^2 + d_1 d_2)}. \quad (19)$$

309 From equations (19) and (18), along with the relations (4) and (5), we can construct all three
 310 components of the velocity field from a diabatic heating source. There only involves one elliptic
 311 inversion to compute Φ from equation (19), a vertical integration of equation (18) to compute ψ

$$\psi = -\frac{2\Omega}{d_1} \int_z^\infty \frac{\partial \Phi}{\partial n} dz' \quad (20)$$

312 where the constant of integration is chosen so that the horizontal velocity vanishes at infinite height,
 313 and a vertical integration of equation (5),

$$w = \int_0^z \nabla_h^2 \Phi dz', \quad (21)$$

314 where the constant of integration is chosen so the vertical velocity vanishes at $z = 0$. Taking the
 315 necessary partial derivatives of Φ and ψ in (4), we have then computed horizontal components of
 316 the velocity field.

317 From the buoyancy equation (3d), we could easily compute b as the deviation of the vertical
 318 velocity from WTG, but this expression would be singular in the radiative damping parameter, d_2 ,
 319 and not illuminating in the WTG limit. Instead, by subtracting the z derivative of the meridional

320 acceleration equation (3c) from the y derivative of the vertical acceleration equation (3d) eliminating ψ using equation (18), and performing some antiderivatives, we arrive at the expression for the
 321 buoyancy in terms of the velocity potential
 322

$$b = -d_1 \int_z^\infty \left[\nabla_h^2 \Phi + \Phi_{zz} + \left(\frac{2\Omega}{d_1} \right)^2 \Phi_{nn} \right] dz', \quad (22)$$

323 where we have chosen the constant of integration so that the buoyancy vanishes at infinite heights.
 324 This equation (22) makes the effect of rotation on buoyancy explicit through the presence of the
 325 last term in the integral, and it will be useful when constructing upscale fluxes for convective
 326 parameterizations. To determine the pressure perturbation, ϕ , we vertically integrate equation
 327 (3c) using the condition that ϕ vanishes at infinite height

$$\phi = \int_z^\infty [d_1 w - 2\Omega \cos(\lambda) u - b] dz'. \quad (23)$$

328 The exact expression for ϕ in terms of Φ or S is not particularly illuminating, so we leave equation
 329 (23) as it is. We note, however, that in the absence of buoyancy and damping, equation (23)
 330 expresses the vertical geostrophic balance discussed by Igel and Biello (2020).

331 *a. Diffusive Momentum Damping*

332 Now we briefly examine the equations when the damping in the momentum equations takes the
 333 form of enhanced turbulent diffusivity. Effectively, this corresponds to replacing the momentum
 334 drag coefficient with the diffusion operator; $d_1 \rightarrow -\mu \nabla^2$ and every instance of d_1 in the denominator
 335 should be interpreted as the inversion of the Laplacian. In this case, the equation for the velocity
 336 potential becomes

$$\left[\left(N^2 - \mu d_2 \nabla^2 \right) \right] \nabla^2 \nabla_h^2 \Phi - \frac{d_2}{\mu} \left[\mu^2 \nabla^4 \Phi_{zz} + (2\Omega)^2 \Phi_{nn} \right] = \nabla^2 S_z. \quad (24)$$

337 The equations for the other variables follow in much the same manner, and we do not record them
 338 here as they don't necessarily provide any more insights into the solutions. However, we note that
 339 in the case of diffusive damping, we must solve elliptic equations for all the variables, whereas for
 340 linear damping we need only solve a single elliptic equation for Φ .

341 4. The Traditional and Non-Traditional Coriolis Terms

342 We now look at the two cases where either only the NCTs or the only the traditional Coriolis
 343 terms (TCTs) are retained in equations (3a)-(3e). The former case occurs at the equator, and is
 344 obtained by setting $\lambda = 0$, and $\partial/\partial n = \partial/\partial y$. The latter case occurs at the north pole, and is
 345 obtained by setting $\lambda = \pi/2$, and $\partial/\partial n = \partial/\partial z$. For the purposes of this discussion, instead of using
 346 the equation for the velocity potential (19), we will recast it in terms of the vertical velocity by
 347 substituting (5).

348 Specifically, at the equator, only the non-traditional Coriolis terms are active, and the elliptic
 349 equation for the vertical velocity becomes

$$[N^2 + d_1 d_2] \nabla_h^2 w + d_1 d_2 \left[w_{zz} + \left(\frac{2\Omega}{d_1} \right)^2 w_{yy} \right] = \nabla_h^2 S, \quad (25)$$

350 while the kinematic equation for the stream function in terms of the velocity potential becomes

$$d_1 \frac{\partial \psi}{\partial z} = 2\Omega \frac{\partial \Phi}{\partial y}. \quad (26)$$

351 There are two cases of note that occur at the equator. In the case of $d_2 = 0$, the equation for the
 352 vertical velocity is independent of latitude, and simplifies to $\nabla_h^2 w = N^{-2} \nabla_h^2 S$, whose solution is
 353 $w = N^{-2} S$. Thus, in the absence of radiative damping, we obtain the WTG approximation (Hittmeir
 354 and Klein 2018), the direct diagnosis of vertical velocity from heating.

355 The second case occurs if both d_1 and d_2 are non-zero, but their product is small enough to
 356 neglect $d_1 d_2$, corresponding to $d_1 d_2 \ll N^2$. In this case, the equation for the vertical velocity at
 357 the equator becomes

$$\nabla_h^2 w + \frac{4\Omega^2}{N^2} \frac{d_2}{d_1} w_{yy} = \frac{1}{N^2} \nabla_h^2 S, \quad (27)$$

358 which is an equation that would allow for the vertical velocity to be diagnosed directly if not for
 359 the term proportional to d_2/d_1 . So in the case of non-zero radiation, we have an equation for the
 360 vertical velocity similar to WTG, but with a modification induced by the presence of radiation and
 361 the non-traditional Coriolis force terms that requires the inversion of an elliptic operator. Thus,
 362 radiation makes the velocity a non-local function of the heating, particularly in the meridional
 363 direction.

364 We point out that there are cases that we have not considered where vertical non-locality induced
 365 by the presence of the w_{zz} term in equation (25) is important (Kuo and Neelin 2022). Our focus,
 366 however, is on the impact of the non-traditional Coriolis terms, which manifest themselves through
 367 the w_{yy} term in equation (25). By considering the case where $d_1 d_2 \ll N^2$, we can isolate the
 368 impact of the NCTs alone.

369 Irrespective of the momentum damping coefficient, at the equator the secondary horizontal
 370 circulation described by ψ is proportional to the meridional derivative of Φ - i.e. the horizontal
 371 circulation induced by the NCT at the equator is proportional to the meridional component of
 372 the poloidal circulation. Thus we expect poloidal flows which are symmetric about the equator to
 373 induce secondary circulations which are antisymmetric about the equator. This symmetry breaking
 374 has important implications for upscale momentum fluxes which we will pursue in future work.

375 At the north pole, the vertical velocity satisfies

$$[N^2 + d_1 d_2] \nabla_h^2 w + d_1 d_2 \left[1 + \left(\frac{2\Omega}{d_1} \right)^2 \right] w_{zz} = \nabla_h^2 S \quad (28)$$

376 and the stream function is proportional to the velocity potential

$$d_1 \psi = 2\Omega \Phi. \quad (29)$$

377 The relationship of the stream function to the velocity potential in equation (29) describes the
 378 well known behavior of geostrophically balanced flows: areas of horizontal convergence of the
 379 poloidal flow will drive cyclonic rotation. Usually this occurs in the lower troposphere where the
 380 flow is convergent, while the compensating, divergent, anticyclonic circulation occurs in the upper
 381 troposphere.

382 In contrast to the NCT equation in (25), where the non-WTG terms (those proportional to d_2)
 383 manifest as both horizontal and vertical derivatives of w in the elliptic operator, in the case of TCT,
 384 given in equation (28), the additional term is only proportional to vertical derivatives of w . This
 385 w_{zz} term generates a vertically non-local response to localized diabatic heating, and it is the effect
 386 of damped gravity waves generated by a convective heating source. The coefficient multiplying the
 387 vertical derivatives in equation (28) is a complicated combination of the rotation rate of the Earth,
 388 the momentum damping, and the ratio of thermal to momentum damping; that is to say that their

389 effects combine in a manner to be indistinguishable from one another in the solution to the vertical
390 velocity.

391 In the companion paper, we will present an extensive study of solutions to the balanced framework.
392 But in order to provide a preliminary illustration of the phenomena that the balanced framework
393 describes, we compute approximate solutions for the velocity potential and stream function at
394 the equator (NCT) and the north pole (TCT), for a horizontally localized heating profile, which
395 maximizes in mid troposphere, thereby resembling the latent heat released by a convective cloud,

$$S = \begin{cases} \frac{S_0}{N^2} \sin(\pi z/H) & \text{if } \sqrt{x^2 + y^2} < L \\ 0 & \text{otherwise,} \end{cases} \quad (30)$$

396 where $S_0 = 10^{-4} \text{ ms}^{-3} = 0.36 \text{ ms}^{-2} \text{ hr}^{-1}$, $H = 3 \text{ km}$, $L = 3 \text{ km}$, and $d_1 = 10^{-4} \text{ s}^{-1}$.

397 Figure 1 (a) shows a horizontal cross section of the secondary circulation, and the vector field
398 $(-\psi_y, \psi_x)$, at the north pole at the bottom of the troposphere, where only the TCT are present. In
399 this case, heating drives a cyclonic secondary circulation whose maximum strength occurs at the
400 bottom and top of the troposphere. Figure 1 (b) shows the secondary circulation at the equator in
401 the middle of the troposphere, when only the non-traditional Coriolis terms are present. In this
402 case, the secondary circulation is antisymmetric about the equator. In figure 1 (c), the velocity
403 potential and vector field $(-\Phi_x, -\Phi_y)$ are plotted at the bottom of the troposphere at the north pole,
404 where only the traditional Coriolis terms are present. Figure 1 (d) shows the velocity potential and
405 vector field $(-\Phi_x, -\Phi_y)$ at the bottom of the troposphere at the equator. In both cases the flow is
406 convergent at the bottom of the troposphere, and divergent at the top.

407 5. Summary

408 In this paper, we discuss a framework for studying convective dynamics under the influence
409 of heating, the full Coriolis force, thermal, and momentum damping. The circulation strengths
410 and length scales we consider allow for the study of steady, linear equilibrated convective flows,
411 and constitutes the first step in studying momentum and buoyancy fluxes from the convective
412 scales to the mesoscales. We use the Helmholtz decomposition of the velocity field as a tool
413 to disentangle the effects of heating, Coriolis force, and damping on the convective circulation,

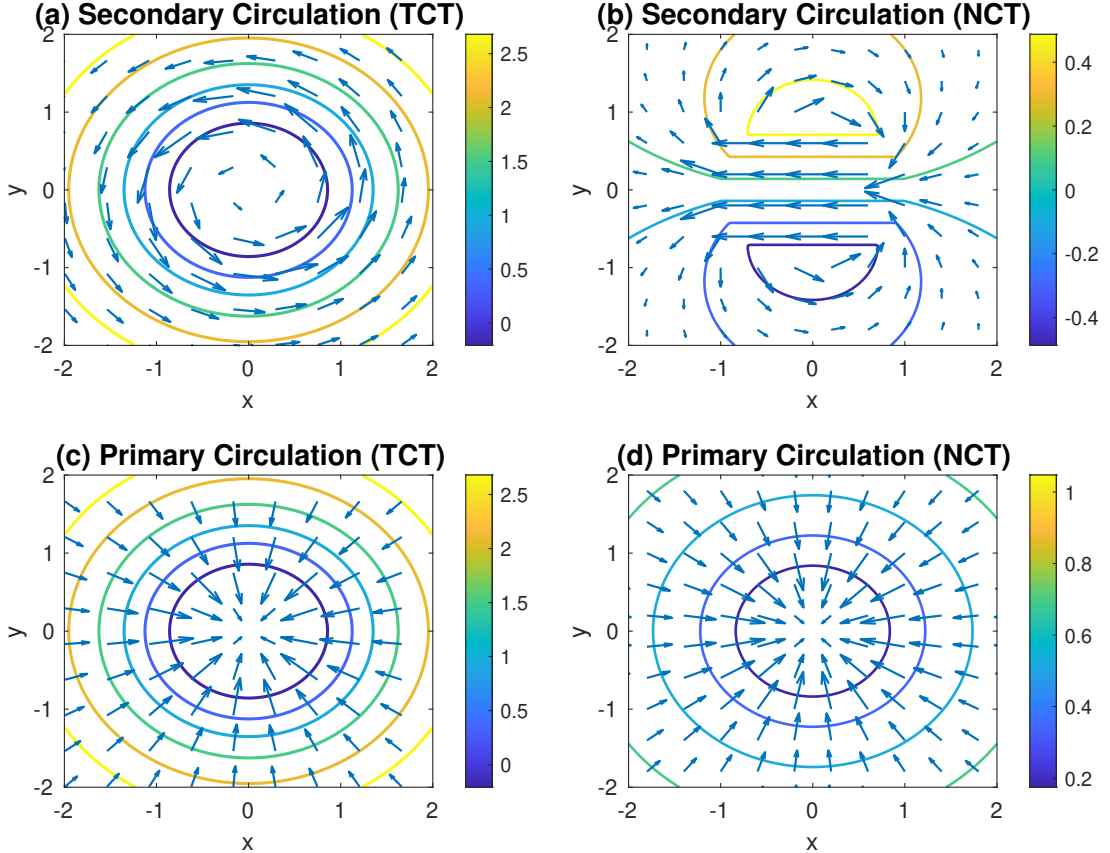


FIG. 1: Figures (a) and (b) show contours of the secondary circulation, ψ , and the vector field $(-\psi_y, \psi_x)$ at the bottom of the troposphere at the north pole, and in the middle of the troposphere at the equator, respectively. Figures (c) and (d) show contours of the velocity potential and the vector field $(-\Phi_x, -\Phi_y)$ at the bottom of the troposphere at the north pole, and at the bottom of the troposphere at the equator, respectively. The axes and variables are scaled to the horizontal length scale, L , and the colorbar is in m/s.

414 $(-\Phi_x, -\Phi_y, w)$, and the secondary horizontal velocity, $(-\psi_y, \psi_x, 0)$, that arises in response to it.
 415 The schematic panels in figure 2 depict (left) the primary convective circulation in the absence of
 416 radiative damping and Coriolis force, (center) the symmetric primary circulation and the rotational
 417 secondary circulation in the presence of radiative damping and the traditional Coriolis force terms,
 418 and (right) the primary and secondary circulation in the presence of radiative damping and the
 419 non-traditional Coriolis force terms.

420 The framework is encapsulated by two equations. The first equation arises from torque balance,
 421 described in (18), which determines the secondary horizontal circulation, ψ , given the velocity
 422 potential. The response of the secondary circulation depends on the latitude of the convection,

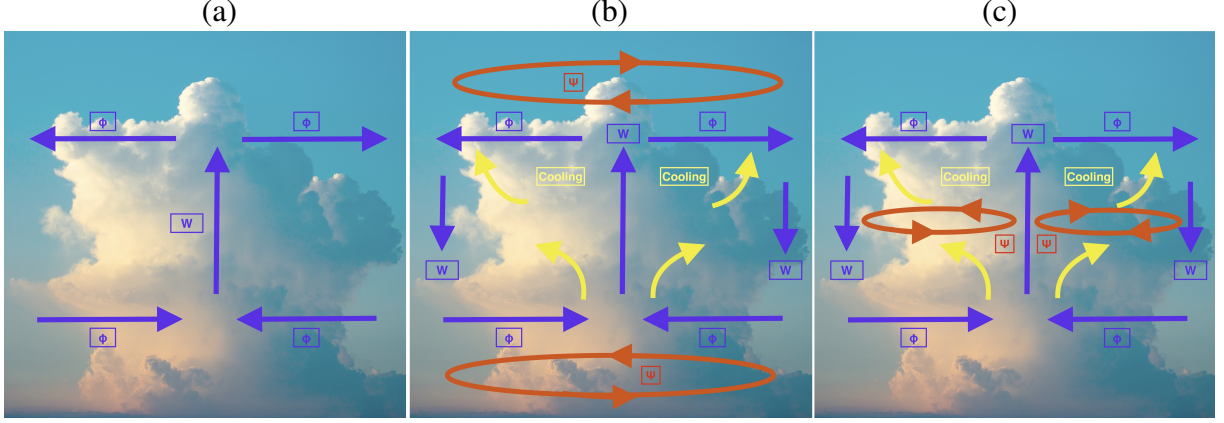


FIG. 2: Schematic representations of the solutions of the convective WTG framework. In purple is the primary poloidal circulation, both the vertical velocity, w , and the horizontal velocity due to the potential, Φ . In yellow is an indication of radiative cooling. Red depicts the secondary circulation ψ , due to the Coriolis force and damping. (a) Shows the WTG without damping or Coriolis force. (b) Shows WTG with radiative cooling and traditional Coriolis terms. (c) Shows WTG with radiative cooling and non-traditional Coriolis terms.

in the absence of the Coriolis terms and radiation, there would only be a poloidal circulation, figure 2 (a). The TCT (poles, figure 2 (b)) drives a cyclonic circulation in response to horizontal convergence, while the NCT (equator, figure 2 (c)) drives an antisymmetric response proportional to the meridional component of the convective velocity field. The red curves in figures 2 (b) and (c) are placed at the heights where the maximum secondary circulation occurs for each case. For the TCT (panel b), equation (29) shows that the the secondary circulation is largest at heights where the horizontal convergence of the convection is largest. From equation (5) we see that this occurs where the vertical derivative of the vertical velocity (and thus the vertical derivative of the heating) is maximum; at the top and bottom of the troposphere. For the NCT (panel c), equation (26) shows the secondary circulation is largest at the height where the meridional velocity of the convection vanishes. At such elevations, the vertical component of the velocity is maximal, therefore the secondary circulation due to the NCT is maximal at the height of the maximum upward velocity in the convection.

The second equation in this framework is an elliptic operator (equation (19)) whose solution yields the velocity potential, Φ , given the diabatic heating, S ; if dissipation is used instead of drag, then the theory is described by equation (24). In the absence of radiative damping, the operator is exactly the weak temperature Gradient approximation, but on convective length scales. Radiative damping generates a response in the vertical component of the velocity field away from the diabatic

⁴⁴¹ heating source, and thus we describe this as a non-local response. In the case of the NCT (equation
⁴⁴² (28)) the non-locality is in the vertical direction (figure 2 (c)) while in the case of the TCT (equation
⁴⁴³ (25)) the non-locality is both in the vertical and meridional directions (figure 2 (b)).

⁴⁴⁴ In a companion paper we study the solutions of this Convective-Coriolis balanced framework.
⁴⁴⁵ Future work will describe the convective momentum and temperature fluxes which arise from
⁴⁴⁶ diabatic heat sources, and the implications of these fluxes for the parameterization of convection
⁴⁴⁷ in meso- and synoptic scale dynamics, especially in the tropics.

448 *Acknowledgments.* This work was partially supported by the NSF under award AGS-2224293.
449 *Data availability statement.* No datasets were generated or analyzed during the current study.

450 **References**

451 Adames, Á. F., S. W. Powell, F. Ahmed, V. C. Mayta, and J. D. Neelin, 2021: Tropical precipitation
452 evolution in a buoyancy-budget framework. *Journal of the Atmospheric Sciences*, **78** (2), 509 –
453 528, <https://doi.org/10.1175/JAS-D-20-0074.1>.

454 Bretherton, C. S., and A. H. Sobel, 2002: A simple model of a convectively coupled walker
455 circulation using the weak temperature gradient approximation. *Journal of Climate*, **15** (20),
456 2907 – 2920, [https://doi.org/10.1175/1520-0442\(2002\)015<2907:ASMOAC>2.0.CO;2](https://doi.org/10.1175/1520-0442(2002)015<2907:ASMOAC>2.0.CO;2).

457 Chikira, M., 2014: Eastward-propagating intraseasonal oscillation represented by
458 chikira–sugiyama cumulus parameterization. part ii: Understanding moisture variation under
459 weak temperature gradient balance. *Journal of the Atmospheric Sciences*, **71** (2), 615–639,
460 <https://doi.org/10.1175/JAS-D-13-038.1>.

461 Dubos, T., C. Barthlott, and P. Drobinski, 2008: Emergence and secondary instability of ekman
462 layer rolls. *Journal of the Atmospheric Sciences*, **65** (7), 2326 – 2342, <https://doi.org/10.1175/2007JAS2550.1>.

464 Helmholtz, H., 1867: On integrals of the hydrodynamical equations, which express vortex-motion.
465 *The London, Edinburgh, and Dublin Philosophical Magazine and Journal of Science*, **33** (226),
466 485–512.

467 Hirt, M., G. C. Craig, and R. Klein, 2023: Scale interactions between the meso- and synoptic
468 scales and the impact of diabatic heating. *Quarterly Journal of the Royal Meteorological Society*,
469 **149** (753), 1319–1334.

470 Hittmeir, S., and R. Klein, 2018: Asymptotics for moist deep convection I: Refined scalings and
471 self-sustaining updrafts. *Theor. & Comput. Fluid Dyn.*, **32**, 137–164.

472 Igel, M. R., and J. A. Biello, 2020: The Nontraditional Coriolis Terms and Tropical Convec-
473 tive Clouds. *Journal of the Atmospheric Sciences*, **77**, 3985–3998, <https://doi.org/10.1175/JAS-D-20-0024.1>.

475 Jeevanjee, N., and D. M. Romps, 2016: Effective buoyancy at the surface and aloft. *Quarterly*
476 *Journal of the Royal Meteorological Society*, **142** (695), 811–820, <https://doi.org/10.1002/qj.2683>.

478 Klein, R., 2010: Scale dependent models for atmospheric flows. *Ann. Rev. Fluid Mech.*, **42** (1),
479 249–274, <https://doi.org/10.1146/annurev-fluid-121108-145537>.

480 Kuo, Y.-H., and J. D. Neelin, 2022: Conditions for convective deep inflow. *Geophysical Research*
481 *Letters*, **49** (20), 1–10.

482 Lebovitz, N. R., 1989: The stability equations for rotating, inviscid fluids: Galerkin methods and or-
483 thogonal bases. *Geophysical & Astrophysical Fluid Dynamics*, **46** (4), 221–243, <https://doi.org/10.1080/03091928908208913>.

485 LeMone, M. A., 1983: Momentum transport by a line of cumulonimbus. *Journal of Atmospheric*
486 *Sciences*, **40** (7), 1815 – 1834, [https://doi.org/10.1175/1520-0469\(1983\)040<1815:MTBALO>2.0.CO;2](https://doi.org/10.1175/1520-0469(1983)040<1815:MTBALO>2.0.CO;2).

488 Manabe, S., and R. F. Strickler, 1964: Thermal Equilibrium of the Atmosphere with a Convective
489 Adjustment. *Journal of the Atmospheric Sciences*, **21** (4), 361–385, [https://doi.org/10.1175/1520-0469\(1964\)021<0361:TEOTAW>2.0.CO;2](https://doi.org/10.1175/1520-0469(1964)021<0361:TEOTAW>2.0.CO;2).

491 Marshall, J., and F. Schott, 1999: Open-ocean convection: Observations, theory, and models.
492 *Reviews of Geophysics*, **37** (1), 1–64, <https://doi.org/10.1029/98RG02739>.

493 Marsico, D. H., J. A. Biello, and M. R. Igel, In Preparation: Balanced convective circulations in a
494 stratified atmosphere. part ii:
495 convective circulations in the presence of radiation and the non-traditional coriolis terms.

496 Ong, H., and P. E. Roundy, 2020: Nontraditional hypsometric equation. *Quarterly Journal of the*
497 *Royal Meteorological Society*, **146** (727), 700–706, <https://doi.org/10.1002/qj.3703>.

498 Ong, H., and D. Yang, 2022: The compressional beta effect and convective system propa-
499 gation. *Journal of the Atmospheric Sciences*, **79** (8), 2031 – 2040, <https://doi.org/10.1175/JAS-D-21-0219.1>.

501 Peters, J. M., 2016: The impact of effective buoyancy and dynamic pressure forcing on vertical
502 velocities within two-dimensional updrafts. *Journal of the Atmospheric Sciences*, **73** (11), 4531
503 – 4551.

504 Raymond, D. J., S. L. Sessions, and Ž. Fuchs, 2007: A theory for the spinup of tropical depressions.
505 *Quarterly Journal of the Royal Meteorological Society*, **133** (628), 1743–1754, <https://doi.org/10.1002/qj.125>.

507 Stewart, A. L., and P. J. Dellar, 2010: Multilayer shallow water equations with complete coriolis
508 force. part 1. derivation on a non-traditional beta-plane. *Journal of Fluid Mechanics*, **651**,
509 387–413, <https://doi.org/10.1017/S0022112009993922>.

510 Stewart, A. L., and P. J. Dellar, 2012: Multilayer shallow water equations with complete coriolis
511 force. part 2. linear plane waves. *Journal of Fluid Mechanics*, **690**, 16–50, <https://doi.org/10.1017/jfm.2011.364>.

513 Stewart, A. L., and P. J. Dellar, 2013: Multilayer shallow water equations with complete coriolis
514 force. part 3. hyperbolicity and stability under shear. *Journal of Fluid Mechanics*, **723**, 289–317,
515 <https://doi.org/10.1017/jfm.2013.121>.

516 Tort, M., and T. Dubos, 2014: Dynamically consistent shallow-atmosphere equations with a
517 complete coriolis force. *Quarterly Journal of the Royal Meteorological Society*, **140** (684),
518 2388–2392, <https://doi.org/10.1002/qj.2274>.

519 Wing, A. A., K. Emanuel, H. C. E., and M. Caroline, 2017: Convective self-aggregation in
520 numerical simulations: A review. *Surveys in Geophysics*, **38**, 1173–1197, <https://doi.org/10.1007/s10712-017-9408-4>.

522 Zhang, K., and G. Schubert, 1997: Linear penetrative spherical rotating convection. *Journal of the
523 Atmospheric Sciences*, **54** (21).